



Faculty of Women for, Arts,
Science, and Education



Scientific Publishing Unit



Journal of Scientific Research in Science

Basic Sciences

Volume 38, Issue 1, 2021

ISSN 2356-8372 (Online) \ ISSN 2356-8364 (print)





Modified Chitosan Hydrogels and Nano Hydrogels for Congo Red Removal from Aqueous System

Shimaa Kh. Farouk^{1,*}, Abir S. Nasr¹, Howida T. Zaky¹, Nadia G. Kandile¹

¹Chemistry Department, Faculty of Women for Art, Science and Education, Ain Shams University, Héliopolis Post Cod. No. 11757, Cairo, Egypt.

Abstract

In the present work, sulfonamide chitosan derivatives were prepared via the reaction of chitosan (Cs) with diphenyl ether - 4, 4'- disulfonylchloride (DPE) in absence and/or presence of glutaraldehyde (G) to form the hydrogel (DPE-I) and (DPE-II) respectively. The nanogels (DPE-III) and (DPE-IV) were prepared via ionotropic gelation method in presence of sodium tri polyphosphate (TPP) under the same reaction conditions. The hydrogels (DPE-I, DPE-II, DPE-III, and DPE- IV) were characterized by different tools as: Elemental analysis, Fourier Transform Infra-Red spectrometer (FT-IR), Proton Nuclear Magnetic Resonance (¹HNMR), Scanning Electron Microscopy (SEM), and Transmission Electron Microscopy (TEM). The adsorption efficiency of the prepared hydrogels for removal of congo red dye (CR) from aqueous solution under different parameters such as (time, pH, and concentration) was evaluated. The adsorption capacity of CR by the prepared hydrogels increased with time, adsorbent dosage and the initial concentration of CR. The optimum adsorption capacity for CR dye by the prepared hydrogels was at pH 7. Hydrogels (DPE-III and DPE-IV) showed the highest efficiency for adsorption of (CR) dye.

Keywords: Chitosan; Diphenyl ether - 4, 4'-disulfonyl chloride; Nanoparticles; Dye removal.

1. Introduction

In recent years, dyes have been one of the most common contaminants in wastewater due to their high toxicity and non-biodegradability [1,2]. CR is toxic to animals and plants and thus its introduction to water stream is seriously hazardous to

***Corresponding author:** Shimaa Kh. Farouk, Chemistry Department, Faculty of Women, Ain Shams University, Heliopolis 11757, Cairo, Egypt.

E-mail: shimaakhaled379@gmail.com

aquatic living organisms and can cause human carcinogen, it was chosen as model dye because of its complex aromatic structure and synthetic nature, it is non-biodegradable and stable under a variety of conditions [3]. CR, a water-soluble anionic dye, has long been used in the printing, textile, leather, cosmetic, and biomedical industries [4].

Common techniques such as membrane separation [5], electrolysis [6], oxidation [7], chemical precipitation [8], adsorption [9,10], photocatalytic degradation [11], biological treatments [12], and flocculation [13] were used to remove dyes from wastewater. The adsorption approach is more appealing for dyes treatment because of its low initial cost, no carcinogenic by-products and high removal efficiency even from dilute solutions [14].

Biopolymers have sparked a lot of interest as adsorbents for wastewater treatment because of the existence of variable chemical reactive groups in polymer chains such as; amino, hydroxyl and acetamido [15].

Chitosan is a biopolymer linear -1, 4-linked polysaccharide that is produced by deacetylation of chitin [16,17]. Due to the unique properties of chitosan made it utilized for a wide range of applications, including wastewater treatment [18], food industry [19], pharmaceutical and biomedical applications [20], and agriculture [21].

Chitosan backbone contains active amine and hydroxyl groups; it can easily be used to remove dyes from wastewater due to its dissolution in acidic environments and weak mechanical properties [3, 22, 23].

As a consequence, chitosan was modified with different crosslinker such as epichlorohydrin or glutaraldehyde to enhance its physicochemical properties for different applications as, biochemical, potential for metals and dyes adsorption from industrial effluents [24].

Chitosan nanoparticles (NPs) are innovative polymeric and bio-based NPs that have a wide range of application, including drug delivery systems, wastewater treatment, food packaging, and agriculture [25]. Various techniques are evaluated to form chitosan NPs such as emulsification, precipitation, reverse micelle ionic gelation

or covalent crosslinking technology [26]. Ionic gelation technique is including anionic cross-linker such as tripolyphosphate (TPP) [27].

Sulfonamides, the most common scaffold in sulfur-containing molecules [28] and used in a wide range of biologically active compounds and medicines containing antimicrobial, anti-inflammatory, anticancer, and protease inhibitors properties [29].

In continuation of our studies [18, 20, 27], chitosan (Cs) was crosslinked with diphenyl ether - 4, 4'-disulfonyl chloride (DPE) under different reaction conditions to form new hydrogels and nanogels to improve its physicochemical properties and its application for dye removal. The new hydrogels were characterized by elemental analysis, (FT-IR), (¹HNMR), (SEM), (TEM). The adsorption efficiency of the new hydrogels for (CR dye) removal from aqueous media under different parameters was studied.

2. Materials and methods

2.1. Materials

Chitosan (Mw = 100 – 300 KDa, DD= 80.5%) (Acros Belgium). Congo Red dye (CR) (Loba Chemie). Glutaraldehyde (G) (Sigma Aldrich) (50% V/V, M.F.= C₅H₈O₂). Dimethylsulfoxide (DMSO) and Chlorosulfonic acid (M.F. = HSO₃Cl, Assay = 99%, Density = 1.75g/mL) were obtained from Alpha. Diphenyl ether ((M.F. = C₁₂H₁₀O, B.P. = 256 °C) and Sodium tri-polyphosphate (TPP) were obtained respectively from Merck and Adwic. Hydrochloric acid (HCl) (Assay = 36.5-38.0%, d = 1.2g/mL) was obtained from Sigma Aldrich. Sodium hydroxide sheets (NaOH) was obtained from El-Gomhouria.

2.2. Methods

2.2.1. Synthesis of diphenyl ether - 4, 4'-disulfonyl chloride (DPE)

A mixture of diphenyl ether (0.05 mol), chlorosulfonic acid (1.5 mol) and urea (0.2 mol) as a catalyst was stirred at 50-60 °C for 4½ h. The solid product was recrystallized from chloroform-n-hexane mixture (1:1), to give white solid, m.p 127 °C (Literature 124-126 °C) [30].

2.2.2. Synthesis of hydrogel Cs

Chitosan (1 g, 1% w/v) was dissolved in aqueous solution of acetic acid (100 mL, 1% v/v) under stirring for 2 h at room temperature. The obtained chitosan hydrogel was washed with (0.1 M) sodium hydroxide solution for neutralization and deionized water then left to dry in air to give hydrogel Cs.

2.2.3. Synthesis of hydrogels DPE-I and DPE-II

Chitosan (0.5g) was dissolved in 60 mL (1% V/V) acetic acid with stirring for 1h. Subsequently, 0.57g of DPE was dissolved in (3mL) DMSO and was added dropwise to chitosan solution. The reaction mixture was stirred at room temperature for 48 h to give (DPE-I) hydrogel, and in presence of glutaraldehyde (5mL, 50% V/V) until gelation to give (DPE-II) hydrogel. Thereafter the reaction mixture was poured into petri dish and left to dry at room temperature. The obtained hydrogels were washed with 0.1M sodium hydroxide solution to neutralize the excess of acetic acid solution and distilled water, then left to dry at room temperature.

2.2.4. Synthesis of nanohydrogels DPE-III and DPE-IV

Chitosan (0.5g) was dissolved in 60 mL (1% V/V) acetic acid with stirring for 1h. Subsequently, 0.57g of DPE was dissolved in (3mL) DMSO and was added dropwise to chitosan solution. TPP solution (20 mL, 1% w/v) was added to the reaction mixture drop by drop and stirred under magnetic stirrer for 48 h at room temperature to give (DPE-III) hydrogel and in presence of glutaraldehyde (5mL, 50% V/V) until gelation to give (DPE-IV) hydrogel. The reaction mixture was poured into petri dish and left to dry at room temperature. The hydrogels formed were washed with 0.1M sodium hydroxide solution and distilled water and left to dry in air at room temperature.

2.3. Characterizations of chitosan and hydrogels DPE-I, DPE-II, DPE-III, and DPE-IV

2.3.1. Elemental analysis

Elemental analysis for chitosan and prepared hydrogels was done by a Perkin-Elmer 2400 C, H, N elemental analyzer. The degree of deacetylation (DD) of Cs and degrees of substitution (DS) of the prepared hydrogels (DPE-I, DPE-II, DPE-III, and

DPE-IV) were calculated by elemental analysis on the basis of (C/N) percentage according to the following equations:

The DD of chitosan was calculated by the following equation [31]:

$$DD = \left(1 - \frac{\frac{C}{N} - 5.145}{6.861 - 5.145} \right) \times 100 \quad (1)$$

Where 5.145 is represented the ratio of C/N of completely N-deacetylated chitosan ($C_6H_{11}O_4N$ repeated unit) and 6.861 is the ratio of C/N of the fully N-acetylated polymer ($C_8H_{13}O_5N$ repeated unit).

While the degree of substitution of chitosan calculated from the following equation [32]:

$$DS = \frac{N - 6.61}{\left(\frac{686}{143 + M} + \frac{392}{185 + M} \right) - 6.61} \times 100 \quad (2)$$

Where, N is the percentage of nitrogen, M is the molecular weight of introduced moiety.

The values 686, 392, 143 and 185 are constants that represent the equation used to calculate the content of the nitrogen into the polymer.

2.3.2. Fourier transform infrared analysis (FTIR)

Fourier Transformed Infrared spectrometer (FTIR, Nicolet iS 10, Thermo Fisher Scientific, in the Central Lab Ain Shams University, Cairo, Egypt) was applied to identify the structures of the prepared hydrogels. The FT-IR spectrum of the prepared hydrogels in the wave number range from 4000 cm^{-1} to 400 cm^{-1} and the test pellets were made by KBr.

2.3.3. Nuclear magnetic resonance analysis (NMR)

The ^1H NMR spectra were recorded on a Varian Mercury VX-300 NMR spectrometer. ^1H NMR spectra were run at 300 MHz in deuterated dimethylsulfoxide (DMSO- d_6).

2.3.4. Scanning electron microscope analysis (SEM)

Scanning electron microscope (SEM) Model Quanta 250 FEG attached with EDX Unit in the Central Lab National Research Center was used for determine the

morphology of the polymers, Cairo, Egypt. The scanning occurred at accelerating voltage 30 kV and magnification 14× up to 1,000,000.

2.3.5. Transmission electron microscope (TEM)

The TEM images of nanoparticles were illustrated by TEM (JEOL-JEM-1200 EX II, in the Central Lab Ain Shams University, Cairo, Egypt) operating at 100 kV and 100 nm.

2.3.6. Swelling behavior

2.3.6.1. Effect of pH

The Swelling behavior of the prepared hydrogels was evaluated using different pH solution in rang (3- 10). (50 mg) of each prepared hydrogel was immersed in (25 mL) of water with pH 3, 7, and 10 at room temperature. After 24 h, the hydrogels were removed and mopped with filter paper to remove excess surface water. Finally, the hydrogels weighted after swelling and calculated the swelling degree by using the following equation [33].

$$\text{Swelling degree (\%)} = \frac{W_s - W_d}{W_s} \times 100 \quad (3)$$

Where; W_d represents the dry weight of the gel specimen and W_s represents the swollen weight of the hydrogels at certain time.

2.4. Dye removal from aqueous solutions

2.4.1. Adsorption study

Congo red was selected to investigate the adsorption performance of the prepared hydrogels (Cs, DPE-I, DPE-II, DPE-III, and DPE-IV). The removal of dyes from aqueous solution was examined by adsorption method [9,10].

The batch adsorption experiments were conducted in 50 mL conical flasks with 10 mL of dye solutions and 100 mg of hydrogel. Then the supernatant was withdrawn and the dye concentration was determined using an Evolution 300 UV–Vis Spectrophotometer at 497 nm [34]. The stock solution having 100 ppm concentration was prepared by dissolving appropriate amount of CR dye and used it in batch experiments by making required dilution.

Various parameters were studied include time, pH, dose, and concentration. The effect of time was examined for different time intervals (5 h - 72 h) at pH 7. The effect of pH was studied using various pH solutions (3–10) mandala 0.1 M HCl or NaOH solution for 48 h. Impact of dosage was illustrated by using various quantity of prepared hydrogels (50–250 mg) at pH 7 for 48 h. The effect of initial dye concentration was investigated using various CR concentrations (10–100 ppm) at pH 7 for 48 h.

The adsorption capacity q_e (mg/g) and removal efficiency of CR dye by hydrogels was determined by the following equation (4) [10]:

$$\text{Removal efficiency} = \frac{C_0 - C_e}{C_0} \times 100 \quad (4)$$

Where C_0 is the initial concentration of CR (ppm), C_e is the concentration of CR at time.

2.4.2. Adsorption isotherm study

The adsorption isotherm is useful to explain the adsorption capacity of dye molecule at equilibrium to the adsorptive substance concentration in solution at constant temperature adsorbent. Adsorption isotherms studies were carried out using two parameter isotherm models Langmuir and Freundlich.

The Langmuir isotherm assumed that adsorption takes place at specific homogeneous sites within the adsorbent and described the formation of a monolayer of the adsorbate on the outer surface of the adsorbent [35]. The Langmuir isotherm parameters are calculated from Eq. (5) and (6), respectively [36].

$$\frac{C_e}{q_e} = \frac{1}{K_L q_m} + \frac{C_e}{q_m} \quad (5)$$

$$R_L = \frac{1}{K_L C_0} \quad (6)$$

Where, q_e is the amount of dye adsorbed at equilibrium time (mg/g), q_m is the maximum adsorption capacity (mg/g), K_L is the isotherm constants for Langmuir (L/mg), R_L is the separation factor,

The Langmuir constants q_m and K_L is the isotherm were determined from the slope and intercept of the linear plot between C_e/q_e against C_e . The separation factor

(R_L) value gives information about the favorability of adsorption process and calculated from Eq. (6). The value of R_L may be either ($R_L > 1$), ($R_L = 1$), or favorable ($0 < R_L < 1$) that's indicated to the unfavorable, linear, and favorable adsorption process respectively [37].

Freundlich adsorption model is based on the multilayer adsorption of adsorbate at the heterogeneous adsorbent surface [38]. The Freundlich isotherm parameters are calculated from Eq. (7) [36].

$$\text{Log } q_e = \text{Log } K_f + \frac{1}{n} \text{Log } C_e \quad (7)$$

Where, K_f is the capacity of the adsorbent, and n is the intensity of adsorption constant for Freundlich.

The Freundlich constants $1/n$ and K_f values can be derived from the slope and intercept of the plot between $\text{log } q_e$ against $\text{log } C_e$, respectively. The value of n may be either $n < 1$, $1 < n < 2$, or $2 < n < 10$, that's indicated to poor, difficult and good adsorption respectively [39].

2.4.3. Reusability study

The reusability of prepared hydrogel (DPE-IV) was determined by adsorption-desorption cycles. The adsorption experiments were carried out using a CR concentration of 30 ppm (10 mL) mixed with hydrogel of 100 mg at pH 7 for 24 h. For desorption, the CR loaded sample was treated with (0.05 M) NaOH solution (10 mL) for 20 min [1]. The adsorption capacity (q_e) (mg/g) was determined by the following equation (8) [10]:

$$q_e = \frac{(C_0 - C_e)V}{m} \quad (8)$$

Where C_0 is the initial concentration of CR (ppm), C_e is the concentration of CR at time t , V is the volume of the solution (L), and m is the dry weight of the hydrogels (g).

2.5. Statistical Analysis

All measurements were expressed in triplicate in each experiment and the data illustrated by the mean value \pm standard deviation and was done by using Microsoft Excel.

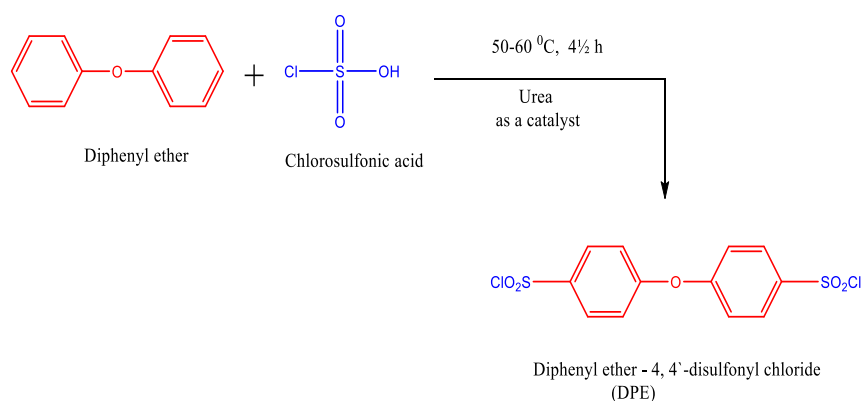
3. Result and discussion

3.1. Synthesis of DPE, DPE-I, DPE-II, DPE-III, and DPE-IV

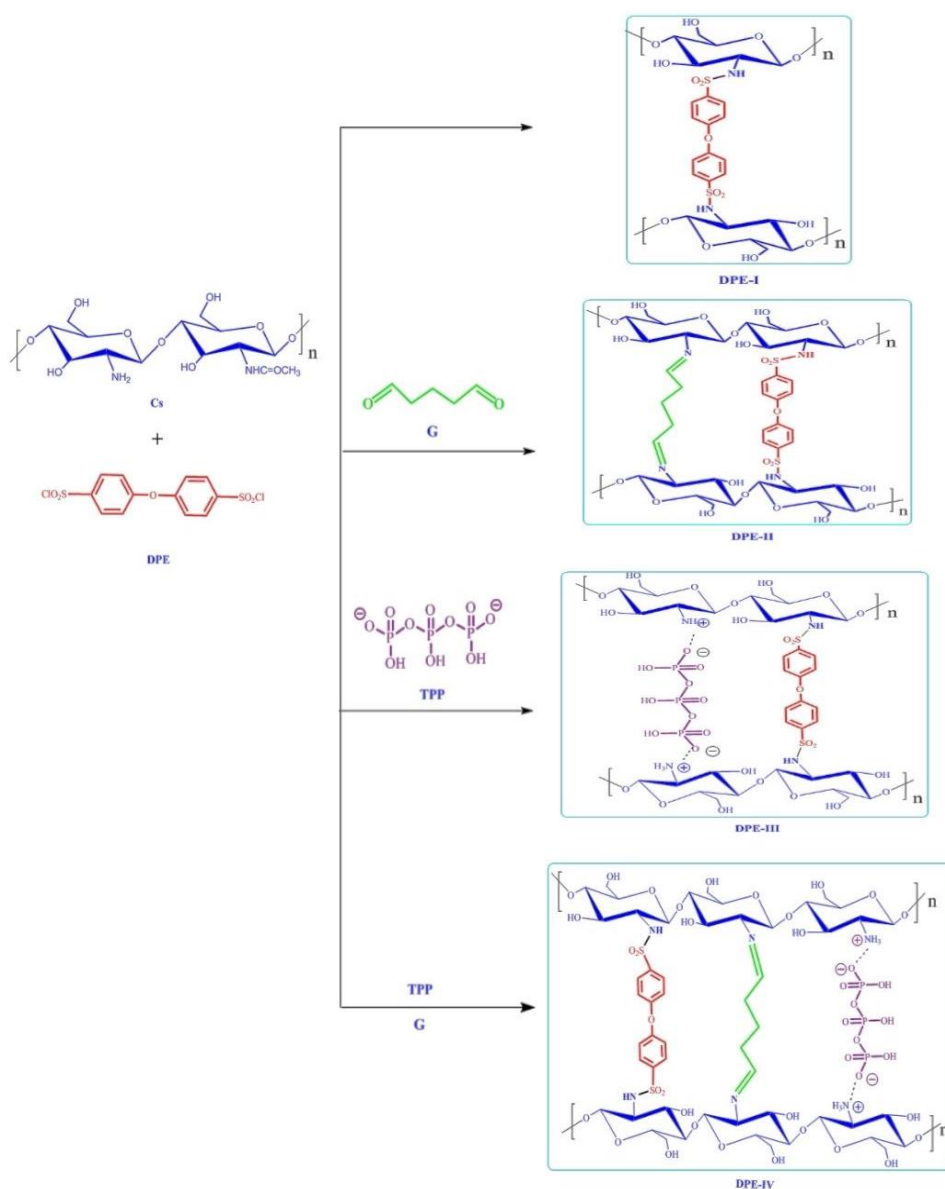
Diphenyl ether - 4, 4'-disulfonyl chloride (DPE) was prepared according to reported procedure [30]. The reaction carried out between diphenyl ether and chlorosulfonic acid in presence of urea as a catalyst as shown in Scheme 1.

Hydrogel DPE-I was synthesized by the reaction of amine groups ($-\text{NH}_2$) of Cs with sulfonyl chloride group ($-\text{SO}_2-\text{Cl}$) of DPE via elimination of HCl. Hydrogel DPE-II was prepared under the same condition in presence of glutaraldehyde as cross-linker Scheme 2.

Nanohydrogels (DPE-III and DPE- IV) were prepared via ionotropic gelation processes through the electrostatic interaction between the positive charge of the protonated amine groups of Cs with the negative charge of TPP in absence or/and presence of glutaraldehyde as shown in Scheme 2 and (Fig.1).



Scheme 1. Synthesis of diphenyl ether - 4, 4'-disulfonyl chloride (DPE)



Scheme 2. Synthesis of hydrogels DPE-I, DPE-II, DPE-III, and DPE- IV

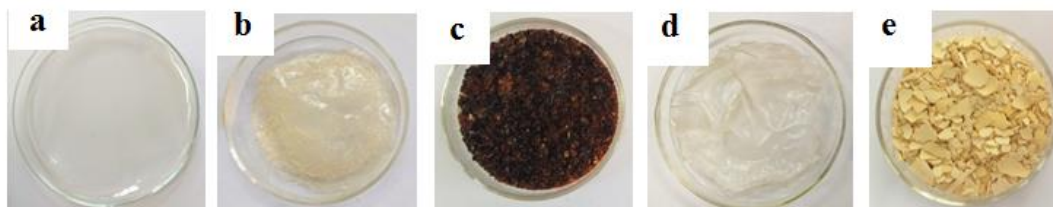


Fig.1. Photographs of hydrogels (a) Cs, (b) DPE-I, (c) DPE-II, (d) DPE-III, and (e) DPE-IV

3.2. Characterization of hydrogels

The structure and morphology of the prepared hydrogels DPE-I, DPE-II, DPE-III, DPE-IV were characterized by elemental analysis, FT-IR, ¹HNMR, SEM, and TEM.

3.2.1. Elemental analysis

The elemental analysis results of hydrogels (Cs, DPE-I, DPE-II, DPE-III, and DPE-IV), expressed as percentages of carbon, nitrogen, hydrogen, and sulphur as well as the carbon/nitrogen ratio, DD% and DS% are listed in Table 1. The results proved that the ratio C/N of the prepared hydrogels was increased with decreasing of nitrogen percentage and increasing DS [34].

The ratio C/N of chitosan and new hydrogels was increased from 5.48 to 9.83, 17.23, 7.98, and 29.12 for DPE-I, DPE-II, DPE-III, and DPE-IV respectively. In case of the hydrogels DPE-II and DPE-IV, the C/N ratio was increased than DPE-I and DPE-III due to the interaction of Cs with the glutaraldehyde.

Table 1

The DD of Cs and DS of the hydrogels DPE-I, DPE-II, DPE-III, and DPE-IV

Prepared hydrogels	Elemental analysis						
	C%	H%	N%	S%	C/N	DD%	DS %
Cs	39.4	17.9	7.2	-	5.48	80.5	-
DPE-I	38.6	14.9	3.9	8.8	9.83	-	58.9
DPE-II	49.5	14.6	2.9	3.9	17.23	-	76.6
DPE-III	35.2	10.7	4.4	5.4	7.98	-	48.3
DPE-IV	52.1	15.2	1.8	2.3	29.12	-	98.7

3.2.2. Fourier transform infrared analysis (FTIR)

The FTIR spectrum of Cs showed a broad peak at 3418 cm^{-1} assigned to OH group and (NH_2) group, while the absorption peaks at 1650 and 1600 cm^{-1} assigned to $\text{C} = \text{O}$ of acetyl group and $\text{N} - \text{H}$ bending of NH_2 , respectively Fig.2 [40].

The FTIR spectrum of hydrogel DPE-I showed peak at 3433 cm^{-1} due to presence of $\text{O} - \text{H}$ implied to the $\text{N} - \text{H}$ stretch. The peaks were appeared at 1637 and 1587 cm^{-1} assigned to $\text{C} = \text{O}$ of acetyl group and bending of $\text{N} - \text{H}$.

Hydrogel DPE-II showed strong peak at 3433 cm^{-1} and was assigned to $\text{O} - \text{H}$ group implied to the $\text{N} - \text{H}$ stretch of Cs. The adsorption band was appeared at 1656 cm^{-1} attributed to $\text{C} = \text{O}$ of acetyl group and $\text{C} = \text{N}$ group results from reaction of glutaraldehyde with chitosan. In addition to, a peak was appeared at 1585 cm^{-1} which assigned to $\text{N} - \text{H}$ bending, this revealed that the glutaraldehyde was crosslinked with Cs.

The FTIR spectrum of hydrogel DPE-III showed strong band at 3435 cm^{-1} due to presence of $\text{O} - \text{H}$ and the $\text{N} - \text{H}$ stretch. The adsorption peaks of $\text{C} = \text{O}$ of acetyl group and $\text{N} - \text{H}$ bending was appeared at 1631 and 1532 cm^{-1} , respectively. New absorption bands were appeared at 1383 cm^{-1} and 1004 cm^{-1} for the $\text{P} = \text{O}$ and $\text{P} - \text{O}$ groups, respectively, which revealed to the formation of strong intermolecular hydrogen bonding between amine groups of chitosan with sodium tripolyphosphate (TPP).

The FTIR spectrum of DPE-IV showed strong peak at 3422 cm^{-1} was assigned to $\text{O} - \text{H}$ group implied to the $\text{N} - \text{H}$ stretch. The adsorption band was appeared at 1636 cm^{-1} attributed to $\text{C} = \text{O}$ of acetyl group and $\text{C} = \text{N}$ group result from reaction of glutaraldehyde with chitosan. In addition to, a peak appeared at 1543 cm^{-1} which assigned to $\text{N} - \text{H}$ bending. New absorption bands were appeared at 1378 cm^{-1} and 1006 cm^{-1} for the $\text{P} = \text{O}$ and $\text{P} - \text{O}$ groups, respectively.

Compared Cs with (DPE-I, DPE-II, DPE-III, and DPE-IV) exhibited five additional peaks at (1491 cm^{-1}), (1303 & 1124 cm^{-1}), and (1247 & 1029 cm^{-1}), which are corresponding to aromatic ring [41], SO_2 group and ether group ($-\text{O}-$) of the DPE moiety respectively, confirming the reaction between Cs and DPE [42, 43].

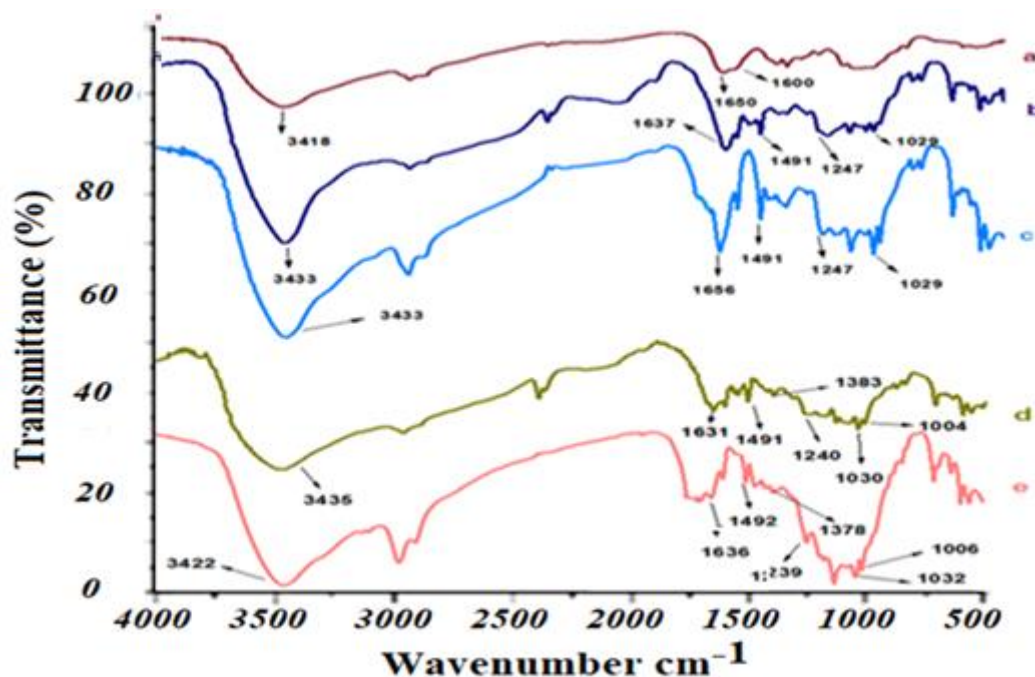


Fig.2. FTIR of hydrogels (a) Cs, (b) DPE-I, (c) DPE-II, (d) DPE-III, (e) DPE-IV

3.2.3. Nuclear magnetic resonance analysis (NMR)

^1H NMR spectrum for hydrogel DPE-I showed the protons at 2.5 ppm (COCH_3), 2.89 ppm (CH_2), 3.74 ppm ($\text{CH}_3 - \text{CH}_6$), 5.06 ppm (OHCH_2), 5.38 ppm (OHCH), 6.98 – 7.65 ppm (4H of ArH), 7.95 ppm for (NHSO_2) and 8.33 ppm (NHCO). The signal of the solvent employed (DMSO-d_6) appears at 3.3 ppm [44, 45] Fig. 3.

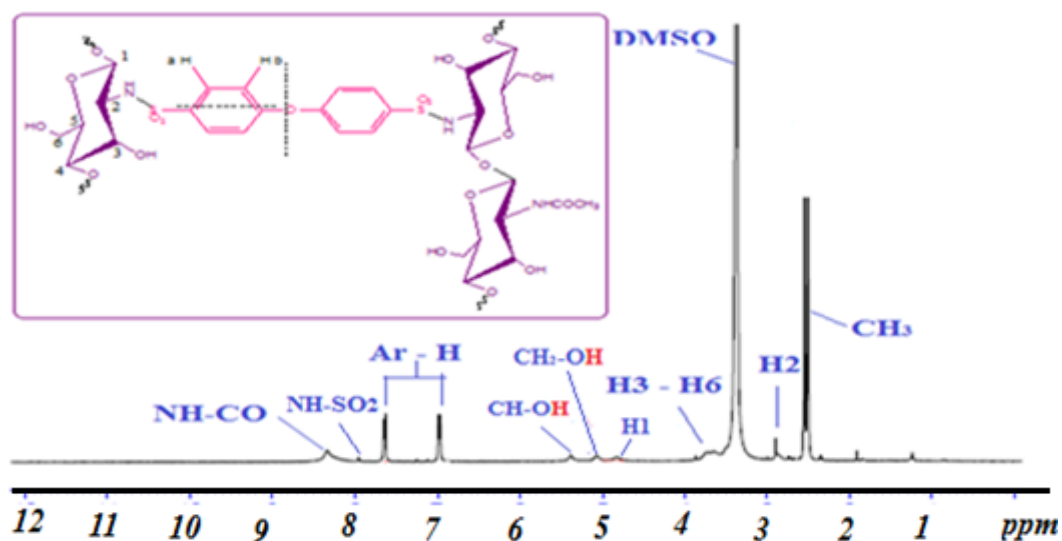


Fig.3. ^1H NMR of DPE-I

3.2.4. Scanning electron microscope (SEM)

The images of morphology of the prepared hydrogels (Cs, DPE-I, and DPE-II) was investigated using SEM at 40 μm magnification and the images are represented in Fig.4(a-c). The surface morphology of Cs was observed as a smooth surface [46], while DPE-I was a smooth surface with small grains due to interaction of Cs with DPE. Compared to Cs, DPE-II had an extremely a rough agglomerated surface and high degree of lumps due to formation of crosslinking hydrogel in presence of glutaraldehyde.

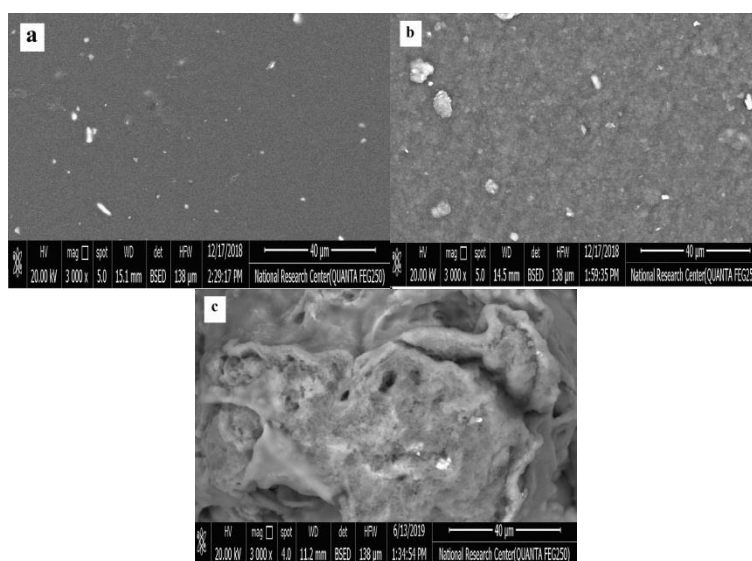


Fig.4. SEM images of (a) Cs, (b) DPE-I, and (c) DPE- II

3.2.5. Transmission Electron Microscopy (TEM)

TEM images of the nano hydrogels DPE-III and DPE- IV were carried out at 100 kV and 100 nm as shown in Fig.5 (a-b). The average nanoparticles size of nanogel DPE-III was found to be 27.9 - 49.2 nm (Fig. 5a) using Magnification at 40000 \times , and for nanogel DPE- IV was found to be 31.3 - 66.5 nm with spherical shapes (Fig. 5b) using Magnification at 40000 \times .

These results confirmed the formation of intermolecular cross-linking between (TPP) and amine groups in Cs and was indicated that the structures of DPE-III and DPE- IV were in nanoscale sizes [47].

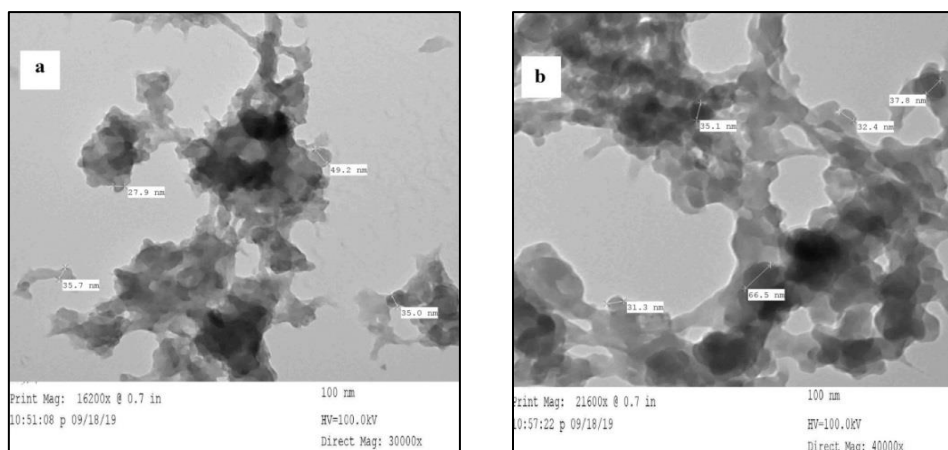


Fig.5. TEM of: (a) DPE-III at Magnification: 30000 \times , (b) DPE-IV at Magnification: 40000 \times .

3.2.6. Swelling behavior

3.2.6.1. Effect of pH

The swelling behavior of the prepared hydrogels (Cs, DPE-I, DPE-II, DPE-III, and DPE-IV) was measured in different pH (3 - 10) at room temperature as shown in Fig.6. The swelling degree was depended on the hydrophilicity and microstructure of the hydrogels. The result obtained revealed that the swelling ratio of all hydrogels decreased as the pH increased [48]. Moreover, at low pH, the amino group of Cs was protonated which allowed more intramolecular hydrogen bonding and penetrated water into the gel network. After crosslinked Cs with DPE and G, the swelling degree of hydrogels decreased due to the formation of crosslinked structure of hydrogels [49].

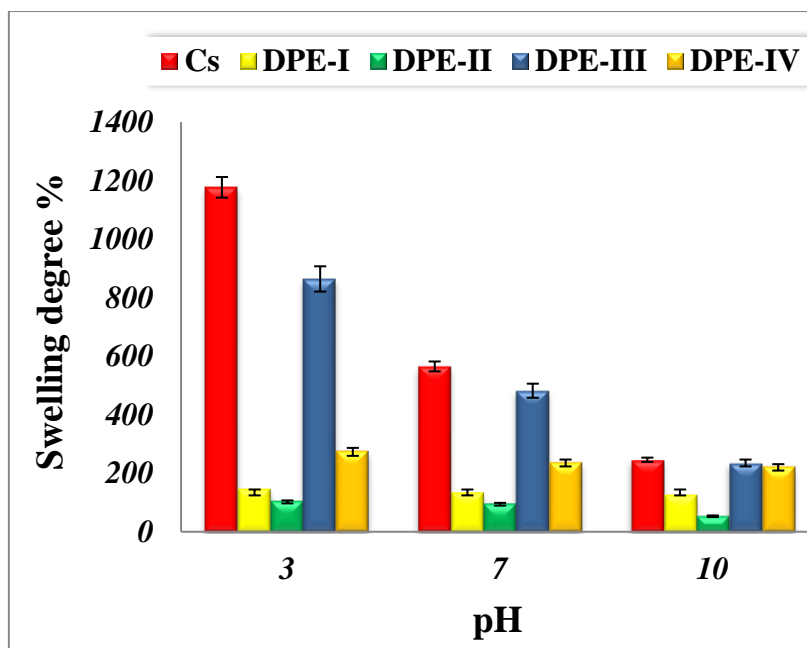


Fig.6. Swelling degree of prepared hydrogels under different pH

3.3. Evaluation of the new hydrogels for Adsorption of Congo Red from aqueous solutions

3.3.1 Influence of contact time

Impact of contact time on the adsorption of CR for prepared hydrogels (Cs, DPE-I, DPE-II, DPE-III, DPE-IV) was examined at different periods of time from 5 to 72 h using an initial concentration of CR (30 ppm), a volume of (10 mL) and a dosage of hydrogels (0.1 g) at pH 7 Fig. 7. The adsorption capacity of CR by the prepared hydrogels was quickly increased through 30 h and after that gradually increased for 72 h. The adsorption of Congo red by hydrogels DPE-I, DPE-III, and DPE-IV needs 30 h to reach equilibrium as compared to hydrogel DPE-II was reached within 50 h. The highest adsorption rate of Congo red by DPE-I, DPE-II, DPE-III, and DPE-IV due to presence of large number of sites were used for adsorption [50]. According to these results, the dye removal efficiency from aqueous solutions for prepared hydrogels (DPE-I, DPE-II, DPE-III, DPE-IV) was superior compared to chitosan, and the nanohydrogels DPE-III, and DPE-IV showed higher results than hydrogels DPE-I, and DPE-II due to the presence of TPP [50]. These results are high compared to other researches such as the results reported with Das L. et al [33].

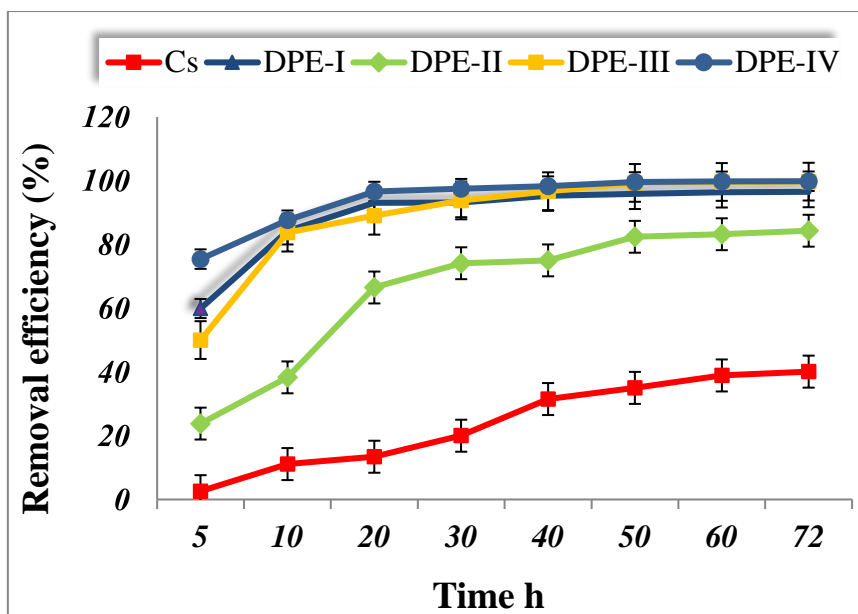


Fig.7. Effect of time on CR absorption

3.3.2. Influence of solution pH

The pH of an aqueous solution is effective on the chemical properties of the adsorbate and adsorbent so it is an important factor for identify the capacity of adsorption of the prepared hydrogels [22]. The effect of pH on the adsorption capacity of chitosan and the prepared hydrogels (DPE-I, DPE-II, DPE-III and DPE-IV) was investigated at pH values (3, 7, and 10), CR solution (30 ppm), in 10 mL volume and 0.1 g of hydrogels for 48 h Fig.8. The optimum adsorption for CR by Cs, DPE-I, DPE-II, DPE-III, and DPE-IV was observed at pH 7, where 31.1 %, 95.8% 78 %, 97.8% and 98.1% adsorption percentages were observed respectively. Due to the solubility of chitosan at pH 3 therefore; the dye removal efficiency is neglectable [3, 23].

From data, dye adsorption efficiency was increased as the pH value of the dye solution was increased due to amine groups of hydrogels will remain fully ionized at pH 7 [51]. But at $\text{pH} < 7$, the amine groups of the hydrogels are not in ionized form resulting in low dye adsorption. Above pH 7, the adsorption of CR was decreased [52].

The adsorption mechanism of the Congo red on the hydrogel depended on electrostatic forces between dye molecule and a protonated amino group of the

hydrogel. At $\text{pH} > 7$, the electrostatic repulsion was increased due to increase of the negative charge density on the surface of the dye molecules, so the adsorption of dye was decreased at $\text{pH} 10$ [53].

Hydrogel DPE-IV was given high adsorption for CR in the range $\text{pH} 3\text{--}10$, so it can be used in wastewater in a wide pH range.

Finally, the result showed that the dye removal efficiency for prepared hydrogels (DPE-I, DPE-II, DPE-III, DPE-IV) was better than chitosan.

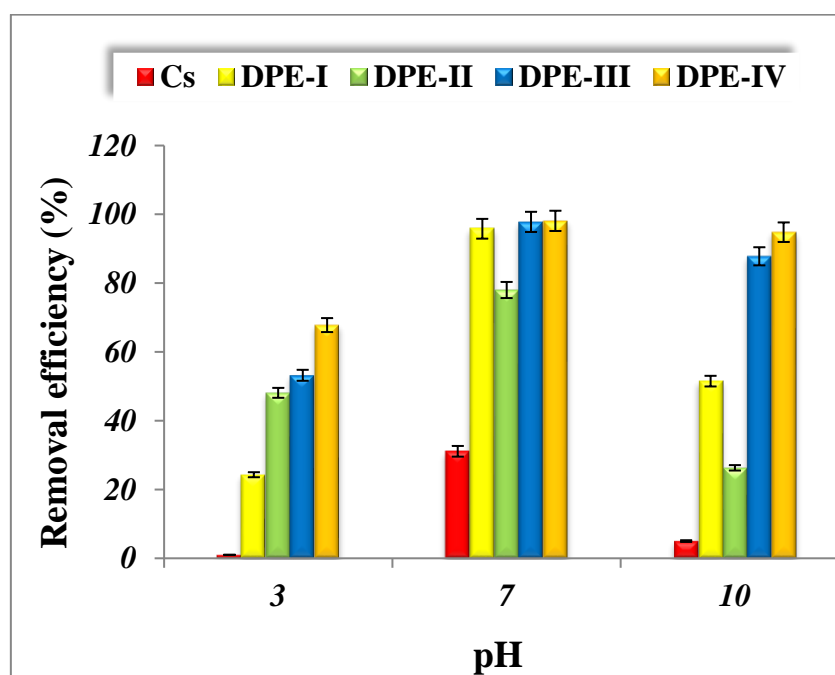


Fig.8. Effect of pH on CR adsorption

3.3.3. Influence of sorbent dose

Sorbent dose of the hydrogels is an important parameter which effect on the removal of CR dye from solution. The effect of dose of prepared hydrogels (Cs, DPE-I, DPE-II, DPE-III, DPE-IV) on adsorption of CR dye was determined by using different doses from 50 to 250 mg at $\text{pH} 7$ and 30 ppm dye solution Fig.9. Generally, the percentage removal of the dye was increased proportionally with increasing adsorbent dosage [54], this is due to as adsorbent increase as the surface area was available for adsorption increase [55]. The results showed that the efficiency removal of CR dye of hydrogels DPE-I, DPE-III and DPE-IV was high ($> 85\%$) at lowest dose (50 mg) then the efficiency of the removal was increased as the dose was increased

until saturation level at dose 200 mg, while in case of hydrogels chitosan and DPE-II, the percentage removal of CR dye was increased sharply from 15.8% to 52.8% and from 53.8% to 89.9 %, respectively at higher dose (250 mg). The optimum adsorption for CR by Cs, DPE-I, DPE-II, DPE-III, and DPE-IV was observed at sorbent dose 100 mg.

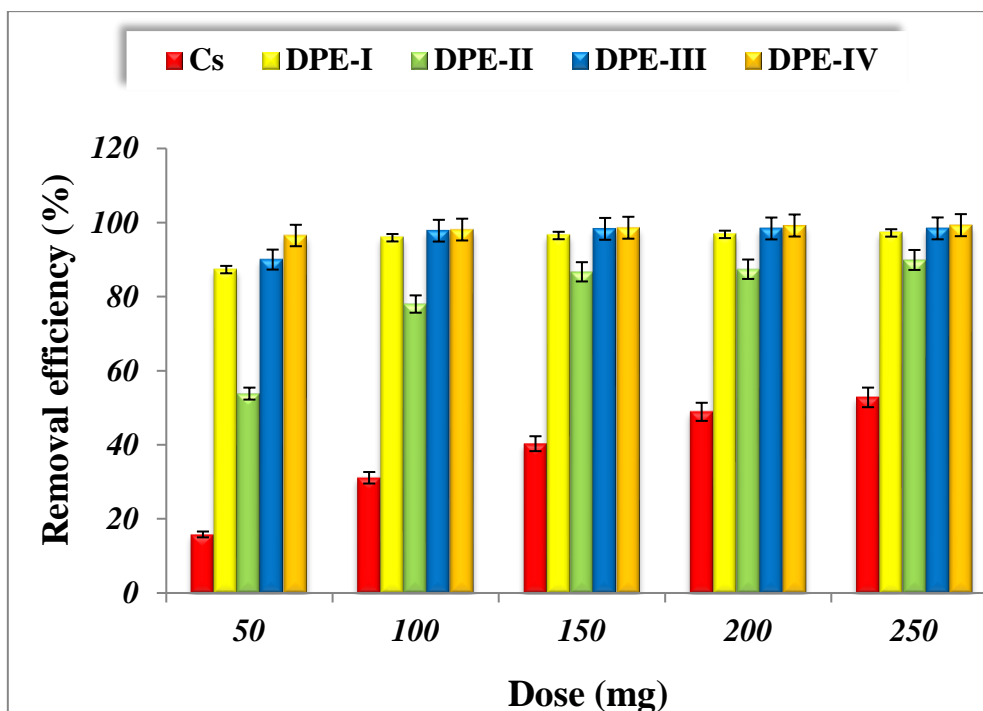


Fig.9. Effect of dose on CR absorption

3.3.4. Influence of CR dye concentration on adsorption

The influence of the initial concentration of CR dye on adsorption was determined by concentration rang of CR from 10 to 100 ppm at pH 7 for 48 h with adsorbent weight (100 mg) Fig.10. The results were showed that the adsorption of CR dye of the prepared hydrogels (DPE-I, DPE-III and DPE- IV) was increased with increasing the initial concentration of CR from 10 to 100 ppm [56, 57]. But in case of hydrogels (chitosan, and DPE-II) by increasing CR dye concentration than 30 ppm, the dye removal efficiency was decreased due to the limited active sites of this hydrogels [58, 59]. The optimum adsorption for CR by Cs, DPE-I, DPE-II, DPE-III, and DPE-IV was observed at CR concentration 30 ppm.

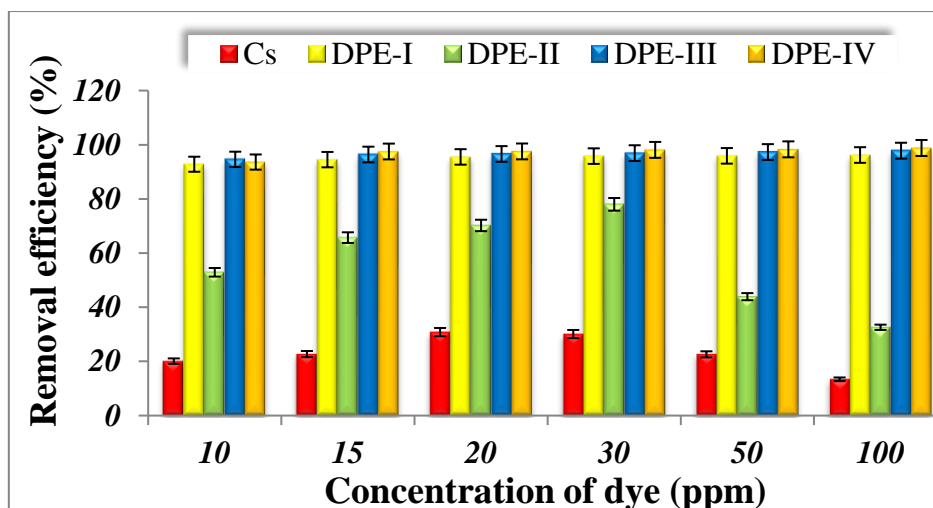


Fig.10. Effect of initial Concentration of CR

3.3.5. Isotherms studies

All the characteristic parameters of both Langmuir and Freundlich for the hydrogel DPE-IV are presented in Table 2. Based on these results, a much higher coefficient constant R^2 of 0.9916 by Langmuir model than 0.9753 by Freundlich model is get. The applicability of the Langmuir isotherm model supports that the adsorption of CR on the surface of the hydrogels occurred by homogeneous monolayer adsorption [33]. In addition, the values of separation factor (R_L) were found to be in the range of 0 –1 ($0.04 \leq R_L \leq 0.15$) indicates that adsorption was favorable. The values of $1/n$ were observed to be 0.9157 for CR dye signifies the adsorption process is favorable [53].

Table 2

Isotherm parameters of hydrogel DPE-IV

Langmuir model				Freundlich model			
Equation	R^2	q_m	K_L	Equation	R^2	$1/n$	K_f
$C_e \setminus q_e = 0.046 C_e + 0.215$	0.9916	21.55	0.215	$\text{Log } q_e = 0.915 \text{ Log } C_e + 0.489$	0.975	0.916	3.087

3.3.6. Reusability study

The reusability of DPE-IV hydrogel was studied using 0.05 M NaOH solution and carried out using a CR concentration of 30 mg/L at pH 7. The adsorption activity

was examined by 10 adsorption–desorption cycles (as shown in Fig.11). The results revealed that the DPE-IV cannot be recovered using NaOH and its adsorption activity was continuously decreased [1].

The adsorption capacity of DPE-IV was still above 1.7 mg/g by removal efficiency 57% up to 7 cycles. Moreover, the CR adsorption capacity and efficiency of DPE-IV hydrogel decreased by increasing number of cycle adsorption to 0.37 mg/g and 12.3 %, respectively at 10th cycle. This result revealed that the breakage of hydrogel chains due to the repeated base treatment during the regeneration process.

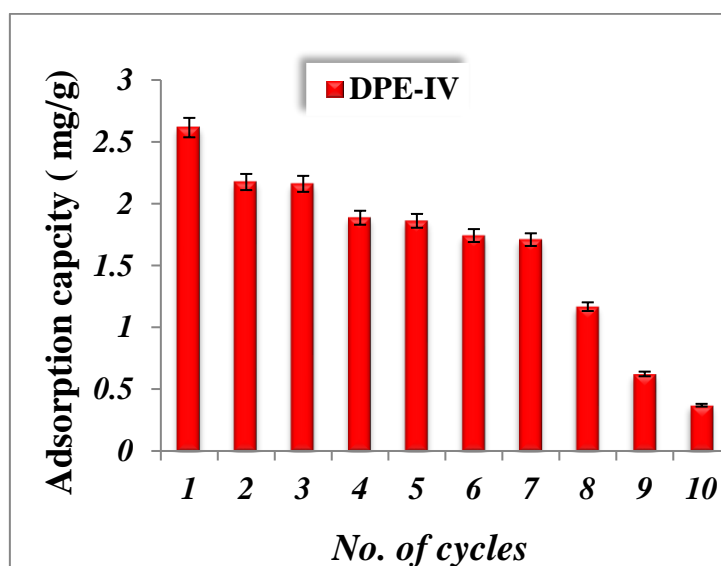


Fig.11. Regeneration study of hydrogel DPE-IV for CR removal for 10 cycles

4. Conclusion

Chitosan-based sulfonamide hydrogels (DPE-I, DPE- II, DPE-III, and DPE-IV) were prepared successfully and applied for CR dye (Congo red) removal from aqueous solutions. Prepared hydrogels were characterized by elemental analysis, FT-IR, ¹HNMR, SEM, and TEM. SEM images showed morphological changes in the surface morphology of the hydrogels (DPE-I, DPE- II) than native chitosan, while TEM for nanoparticles (DPE-III and DPE- IV) indicated particle size in their structures with spherical shapes. The prepared hydrogels (DPE-I, DPE- II, DPE-III, and DPE- IV) were evaluated for CR dye removal using various parameters include time, pH, and concentration. The results of dye removal study showed that the adsorption capacity of CR onto prepared hydrogels (DPE-I, DPE- II, DPE-III, and

DPE-IV) increased with time gradually. In case of different pH values study, the optimum adsorption capacity for CR dye by the prepared hydrogels was observed at pH 7, while the removal efficiency increased by increasing dose of adsorbent and concentration of CR dye.

Declaration of Competing Interest

Authors have declared no conflict of interest for publication of this work.

Acknowledgments

Authors gratefully acknowledge Ain Shams University for samples analysis for this research.

References

- [1] U. J. Kim, S. Kimura, M. Wada, Highly enhanced adsorption of Congo red onto dialdehyde cellulose-crosslinked cellulose-chitosan foam, *Carbohydr. Polym.* 214:(2019) 294-302.
- [2] H. F. Mohamed, B. M. Awad, S. Abd El RahmanI, M. M. El-Sayed, Purification of Industrial Wastewater from Methylene Blue (MB) Dye Using Organic and Inorganic Sol-gel Glasses. *J. Sci. Res. Sci.*, 35:(2018) 400-416.
- [3] R. Huang, L. Zhang, P. Hu, J. Wang, Adsorptive removal of Congo red from aqueous solutions using crosslinked chitosan and crosslinked chitosan immobilized bentonite, *Int. J. Biol. Macromol.* 86:(2016) 496–504.
- [4] Y. Wang, X. Dai, Y. Zhan, X. Ding, M. Wang, X. Wang, In situ growth of ZIF-8 nanoparticles on chitosan to form the hybrid nanocomposites for high-efficiency removal of Congo Red, *Int. J. Biol. Macromol.* 137: (2019) 77-86.
- [5] T. Tavangar, M. Karimi, M. Rezakazemi, K. R. Reddy, T. M. Aminabhavi, Textile waste, dyes/inorganic salts separation of cerium oxide-loaded loose nanofiltration polyethersulfone membranes, *Chem. Eng. J.* 385: (2020) 123787.
- [6] H. Jalife-Jacobo, R. Feria-Reyes, O. Serrano-Torres, S. Gutiérrez-Granados, J. M. Peralta-Hernández, Diazo dye Congo Red degradation using a Boron-doped diamond a node: An experimental study on the effect of supporting electrolytes, *J. Hazard. Mater.* 319: (2016) 78-83.
- [7] Z. Cheng, L. Zhang, X. Guo, X. Jiang, T. Li, Adsorption behavior of direct red 80 and congo red onto activated carbon/surfactant: process optimization, kinetics and equilibrium, *Spectrochim. Acta A Mol. Biomol. Spectrosc.* 137: (2015) 1126–1143.
- [8] A. S. Eltaweil, H. M. Elshishini, Z. F. Ghatass, G. M. Elsubruiti, Ultra-high adsorption capacity and selective removal of Congo red over aminated graphene oxide modified Mn-doped UiO-66 MOF, *Powder Technol.* 379: (2021) 407-416.
- [9] S. Zhuang, K. Zhu, J. Wang, Fibrous chitosan/cellulose composite as an efficient adsorbent for Co (II) removal, *J. Clean. Prod.* 285: (2021) 124911.

- [10] Y. Yue, Z. Peng, W. Wang, Y. Cai, F. Tan, X. Wang, X. Qiao, Facile preparation of MgO-loaded SiO₂ nanocomposites for tetracycline removal from aqueous solution, *Powder Technol.* 347: (2019) 1-9.
- [11] N. Ali, A. Said, F. Ali, F. Raziq, Z. Ali, M. Bilal, H. M. Iqbal, Photocatalytic degradation of congo red dye from aqueous environment using cobalt ferrite nanostructures: development, characterization, and photocatalytic performance, *Water Air Soil Pollut.* 231:(2020) (2) 1-16.
- [12] F. Bosco, C. Mollea, B. Ruggeri, Decolorization of Congo Red by *Phanerochaete chrysosporium*: the role of biosorption and biodegradation, *Environ. Technol.* 38.20: (2017) 2581-2588.
- [13] U. Habiba, T.A. Siddique, T.C. Joo, A. Salleh, B.C. Ang, A.M. Afif, Synthesis of chitosan/polyvinyl alcohol/zeolite composite for removal of methyl orange, Congo red and chromium(VI) by flocculation/adsorption, *Carbohydr.Polym.* 157:(2017) 1568–1576.
- [14] R. Foroutan, R. Mohammadi, S. Farjadfard, H. Esmaeili, B. Ramavandi, Characteristics and performance of Cd, Ni, and Pb bio-adsorption using *Callinectes sapidus* biomass: real wastewater treatment, *Environ. Sci. Pollut. Res.* 26 :(2019) 6336–6347.
- [15] N. Joly, D. Ghemati, D. Aliouche, P. Martin, Interaction of Metal Ions with Mono-and Polysaccharides for Wastewater Treatment: A Review. *Nat Prod Chem Res* 8 :(2020) 373.
- [16] N. El-Tohamy, S. M. Easa, M. Attia, N. M. Awad, Characterization and evaluation of nanocomposites chitosan-multiwalled carbon nanotubes as broad-spectrum antibacterial agent, *J. Sci. Res. Sci.*, 35: (2018) 16-27.
- [17] D. Vallejo-Domínguez, E. Rubio-Rosas, E. Aguila-Almanza, H. Hernández-Cocoletzi, M. E. Ramos-Cassellis, M. L. Luna-Guevara, P. L. Show, Ultrasound in the deproteinization process for chitin and chitosan production, *Ultrasonics Sonochemistry* 72: (2021) 105417.
- [18] N. G. Kandile, H. M. Mohamed, Chitosan nanoparticle hydrogel based sebacyl moiety with remarkable capability for metal ion removal from aqueous systems, *Int. J. Biol. Macromol.* 122: (2019) 578-586.
- [19] H. Wang, J. Qian, F. Ding, Emerging chitosan-based films for food packaging applications, *J. Agric. Food Chem.* 66: (2018) 395–413.
- [20] N. G. Kandile, M. I. Mohamed, H. T. Zaky, A. S. Nasr, Y. G. Ali, Quinoline anhydride derivatives cross-linked chitosan hydrogels for potential use in biomedical and metal ions adsorption, *Polym. Bull.* (2021) 1-26.
- [21] M. Malerba, R. Cerana, Recent advances of chitosan applications in plant, *Polym. (Basel)* 10:(2018) 118.
- [22] S. Chatterjee, H.N. Tran, O.B. Godfred, S.H. Woo, Supersorption capacity of anionic dye by newer chitosan hydrogel capsules via green surfactant exchange method, *ACS Sustain. Chem. Eng.* 6 (3): (2018) 3604–3614.

- [23] X. Zheng, X. Li, J. Li, L. Wang, W. Jin, Y. Pei, K. Tang, Efficient removal of anionic dye (Congo red) by dialdehyde microfibrillated cellulose/chitosan composite film with significantly improved stability in dye solution, *Int. J. Biol. Macromol.* 107: (2018) 283–289.
- [24] S. Omid, A. Kakanejadifard, Eco-friendly synthesis of graphene-chitosan composite hydrogel as efficient adsorbent for Congo red, *RSC Adv.* 8.22 :(2018) 12179-12189.
- [25] M. T. Elshamy, S. M. Hussein, K. Y. Farroh, Application of nano-chitosan NPK fertilizer on growth and productivity of potato plant, *J. Sci. Res. Sci.*, 36(1): (2019)424-441.
- [26] S. Rashki, K. Asgarpour, H. Tarrahimofrad, M. Hashemipour, M. S. Ebrahimi, H. Fathizadeh, H. Mirzaei, Chitosan-based nanoparticles against bacterial infections, *Carbohydr. Polym.* (2020) 117108.
- [27] N. G. Kandile, H. M. Mohamed, New chitosan derivatives inspired on heterocyclic anhydride of potential bioactive for medical applications, *Int. J. Biol. Macromol.* 182:(2021)1543-1553.
- [28] P. Sharma, P. Awasthi, Synthesis, Characterization, In vivo, Molecular Docking, ADMET and HOMO-LUMO study of Juvenile Hormone Analogues having sulfonamide feature as an Insect Growth Regulators, *J. Clean. Prod.* 285 :(2021) 125483.
- [29] T.C. Das, S.A. Quadri, M. Farooqui, Recent advances in synthesis of sulfonamides: A review. *J. Chem. Biol. Interfaces* 8:(2018) 194-204.
- [30] B. Boer, H. Meng, F. Dmitrii, Perepichka, J. Zheng, M. M. Frank, Y. J. Chabal, Z. Bao, Synthesis and characterization of conjugated mono and dithiol oligomers and characterization of their self-assembled monolayers, *Langmuir* 19 :(2003), 4272-4284.
- [31] N.G. Kandile, H.T. Zaky, M.I. Mohamed, A.S. Nasr, Y. G. Ali, Extraction and Characterization of Chitosan from Shrimp Shells, *Open J. Org. Polym. Mater.* 8 (2018) 33-42.
- [32] U. Jančiauskaitė, R. Makuška, Polyelectrolytes from natural building blocks: synthesis and properties of chitosan-O-dextran graft copolymers, *Chemija* 19(2) :(2008) 35-42.
- [33] L. Das, P. Das, A. Bhowal, C. Bhattacharjee, Synthesis of hybrid hydrogel nano-polymer composite using Graphene oxide, Chitosan and PVA and its application in waste water treatment, *Environ. Technol. Innov.* 18 :(2020) 100664.
- [34] E. Alver, M. Bulut, A. Ü. Metin, H. Çiftçi, One step effective removal of Congo Red in chitosan nanoparticles by encapsulation, *Spectrochim. Acta A Mol. Biomol. Spectrosc.* 171: (2017), 132–138.
- [35] T.A. Khan, E.A. Khan, Removal of basic dyes from aqueous solution by adsorption onto binary iron-manganese oxide coated kaolinite: nonlinear isotherm and kinetics modeling, *Appl. Clay Sci.* 107: (2015), 70 -77.

- [36] S. M. R. Goddeti, M. Bhaumik, A. Maity, S. S. Ray, Removal of Congo red from aqueous solution by adsorption using gum ghatti and acrylamide graft copolymer coated with zero valent iron, *Int. J. Biol. Macromol.* 149: (2020) 21–30.
- [37] Y. Ren, H.A. Abbood, F. He, H. Peng, K. Huang, Magnetic EDTA-modified chitosan/SiO₂/Fe₃O₄ adsorbent: Preparation, characterization, and application in heavy metal adsorption, *Chem. Eng. J.* 226: (2013) 300-311.
- [38] M.L. Masheane, L.N. Nthunya, S.P. Malinga, E.N. Nxumalo, S.D. Mhlanga, Chitosan based nanocomposites for de-nitrification of water, *J. Phys. Chem. Earth* (2016) 1–13.
- [39] B. Tanhaei, A. Ayati, M. Lahtinen, M. Sillanpää, Preparation and Characterization of a Novel Chitosan/Al₂O₃/Magnetite Nanoparticles Composite Adsorbent for Kinetic, Thermodynamic and Isotherm Studies of Methyl Orange Adsorption, *Chem. Eng. J.* 259: (2015) 1-10.
- [40] A.M. Youssef, H. Abou-yousef, S.M. El-sayed, S. Kamel, Mechanical and antibacterial properties of novel high-performance chitosan/nanocomposite films, *Int. J. Biol. Macromol.* 76 :(2015) 25–32.
- [41] N.T.Q. Chi, D.X. Luu, D. Kim, Sulfonated poly (ether ether ketone) electrolyte membranes cross-linked with 4,4'-diaminodiphenyl ether, *Solid State Ion.* 187 :(2011) (1), 78–84.
- [42] Y. Liu, Z. Li, J. Zhang, H. Zhang, H. Fan, M. Run, Polymerization behavior and thermal properties of benzoxazine based on 4,4'- diaminodiphenyl ether, *J. Therm. Anal. Calorim.* 111(2): (2013)1523–1530.
- [43] X.S. Wang, Q.F. An, Q. Zhao, K.R. Lee, J.W. Qian, C.J. Gao, Preparation and pervaporation characteristics of novel polyelectrolyte complex membranes containing dual anionic groups, *J. Membr. Sci.* 415 :(2012) 145-152.
- [44] P. K. Panda, J. M. Yang, Y. H. Chang, W. W. Su, Modification of different molecular weights of chitosan by p-Coumaric acid: Preparation, characterization and effect of molecular weight on its water solubility and antioxidant property, *Int. J. Biol. Macromol.* 136 :(2019) 661–667.
- [45] S. Supapvanich, W. Anan, V. Chimsonthorn, Efficiency of combinative salicylic acid and chitosan preharvest-treatment on antioxidant and phytochemicals of ready to eat daikon sprouts during storage, *Food Chem.* 284(2019), 8–15.
- [46] K. S. Sarojini, M. P. Indumathi, G.R. Rajarajeswari, Mahua oil-based polyurethane/chitosan/nano ZnO composite films for biodegradable food packaging applications, *Int. J. Biol. Macromol.* 124: (2019) 163–174.
- [47] M. S. Alhumaimess, I. H. Alsohaimi, A. A. Alqadami, M. A. Khan, M. M. Kamel, O. Aldosari, M. R. Siddiqui, A. E. Hamedelniei, Recyclable glutaraldehyde cross-linked polymeric tannin to sequester hexavalent uranium from aqueous solution, *J. Mol. Liq.* 281 :(2019) 29–38.
- [48] M. Rasoulzadehzali, H. Namazi, Facile preparation of antibacterial chitosan/graphene oxide-Ag bio-nanocomposite hydrogel beads for controlled release of doxorubicin, *Int. J. Biol. Macromol.* 116 :(2018) 54–63.

- [49] O. U. Akakuru, B. O. Isiuku, Chitosan Hydrogels and their Glutaraldehyde-Crosslinked Counterparts as Potential Drug Release and Tissue Engineering Systems - Synthesis, Characterization, Swelling Kinetics and Mechanism, *J Phys Chem Biophys.* 7: (2017) 256.
- [50] R. A. Elzamly, H. M. Mohamed, M. I. Mohamed, H. T., Zaky, D. R. Harding, N. G. Kandile, New sustainable chemically modified chitosan derivatives for different applications: Synthesis and characterization, *Arab. J. Chem.* 14(8): (2021) 103255.
- [51] J. Maity, S. K. Ray, Enhanced adsorption of methyl violet and congo red by using semiand full IPN of polymethacrylic acid and chitosan, *Carbohydr. Polym.* 104 :(2014) 8–16.
- [52] X. Xu, J. Yu, C. Liu, Xanthated chitosan/cellulose sponges for the efficient removal of anionic and cationic dyes, *React. Funct. Polym.* 160: (2021) 10484.
- [53] S. A. Bhat, F. Zafar, A. H. Mondal, A. U. Mirza, Q. M. R. Haq, and N. Nishat, Efficient removal of Congo red dye from aqueous solution by adsorbent films of polyvinyl alcohol/melamine formaldehyde composite and bactericidal effects. *J. Clean. Prod.*, 255:(2020) 120062.
- [54] Z. Zhang, L. Moghaddam, I. M. O'Hara, W. O. S. Doherty, Congo Red adsorption by ball-milled sugarcane bagasse, *Chem. Eng. J.* 178:(2011), 122–128.
- [55] P. Kumar, S. Ramalingam, C. Senthamarai, M. Niranjanaa, P. Vijayalakshmi, S. Sivanesan, Adsorption of dye from aqueous solution by cashew nut shell: studies on equilibrium isotherm, kinetics and thermodynamics of interactions, *Desalination* 261: (2010) 52–60.
- [56] Y. Zheng, Y. Zhu, A. Wang, Highly efficient and selective adsorption of malachite green onto granular composite hydrogel, *Chem.Eng. J.* 1 257: (2014) 66-73.
- [57] H. W. Kwak, M. S. Shin, H. Yun, K. H. Lee, Preparation of silk sericin/lignin blend beads for the removal of hexavalent chromium ions, *Int. J. of Mol. Sci.* 17:(2016), 1466.
- [58] T. Santhi, S. Manonmani, T. Smitha, Kinetics and isotherm studies on cationic dyes adsorption onto annona squamosa seed activated carbon, *Int. J. Eng. Sci. Technol.* 2.3: (2010): 287-295.
- [59] S. Zwane, M. L. Masheane, A. T. Kuvarega, G. D. Vilakati, B. B. Mamba, H. Nyoni, D. S. Dlamini, Polyethersulfone/Chromolaena odorata (PES/CO) adsorptive membranes for removal of Congo red from water, *J. Water Process. Eng.* 30: (2019) 100498.

الملخص باللغة العربية

هيدروجيلات ونانوهيدروجيلات الكيتوزان المعدلة لإزالة صبغة الكونغو الأحمر من الوسط المائي

شيماء خالد فاروق¹ - عبير صلاح نصر¹ - هويدا طلعت ذكي¹ - نادية غريب قنديل¹

1. قسم الكيمياء - كلية البنات للأداب والعلوم والتربية - جامعة عين شمس - القاهرة - جمهورية مصر العربية

في العمل الحالي، تم تحضير مشتقات الكيتوزان سلفوناميد عن طريق تفاعل الكيتوزان مع ثنائي فينيل الإيثر - 4 ، 4 - ثنائي السلفونيل كلوريد في غياب و / أو وجود الجلوتارالدهيد لتكوين الهيدروجيلات (DPE-I) و (DPE-II) على التوالي.

كما تم تحضير النانوجيلات (DPE-III) و (DPE-IV) في وجود ثلاثي فوسفات الصوديوم تحت نفس ظروف التفاعل.

تم توصيف الهيدروجيلات (DPE-I , DPE- II , DPE- III , DPE-IV) بواسطة مقاييس مختلفة مثل: تحليل العناصر و التحليل الطيفي بالأشعة تحت الحمراء (FT-IR) ، بروتون الرنين المغناطيسي النووي (¹HNMR) ، المسح المجهر الإلكتروني (SEM) ، و المجهر الإلكتروني للإنتقال (TEM)، وقد تم تقييم قدرة امتصاص الهيدروجيلات المحضرة لإزالة صبغة CR من المحلول المائي بواسطة عوامل مختلفة تشمل (الوقت ، درجة الحموضة ، والتركيز). كما زادت قدرة امتصاص CR بواسطة الهيدروجيلات المحضرة بزيادة الوقت و جرعة الممتز وتركيز الصبغة، ووجد أن قدرة الامتصاص المثلى لصبغة CR بواسطة الهيدروجيلات المحضرة عند الرقم الهيدروجيني 7 ولقد أظهرت الهيدروجيلات (DPE-I) و (DPE-IV) أعلى كفاءة لامتصاص صبغة CR.